Crystallization of sodium molybdate-phosphate and tungstate-phosphate glasses

Ladislav Koudelka, Oksana Kupetska, Petr Kalenda, Petr Mošner, Lionel Montagne, Bertrand Revel

Crystallization of sodium molybdate-phosphate and tungstate-phosphate glasses

Ladislav Koudelka[1]*, Oksana Kupetska[1], Petr Kalenda[1], Petr Mošner[1], Lionel Montagne[2], Bertrand Revel[2]
[1]*Department of General and Inorganic Chemistry, Faculty of Chemical Technology, University of Pardubice, 532 10 Pardubice, Czech Republic*
[2]*University of Lille, CNRS, Centrale Lille, ENSCL, Univ. Artois, UMR 8181 - UCCS - Unité de Catalyse et Chimie du Solide, F-59000 Lille, France*

Abstract

Study of the glass to crystal transformation was realized for two glasses with composition $25Na_2O.50MoO_3.25P_2O_5$ and $25Na_2O.50MoO_3.25P_2O_5$. During the heat treatment process, 2 crystalline compounds are formed, $NaMoO_2PO_4$ and $NaWO_2PO_4$, respectively. Physico-chemical properties of the corresponding glasses and crystals were compared, as well as their Raman and ^{31}P MAS NMR spectra. DTA studies revealed crystallization peaks at 483°C in the Mo-containing glass and at 624°C in the W-containing glass; melting points of crystalline compounds were determined as 695 ±2°C for $NaMoO_2PO_4$ and 875±2°C for $NaMoO_2PO_4$. Sodium tungstate-phosphate glass has lower solubility in comparison with the sodium molybdate-phosphate glass. The study of crystallization mechanism showed a prevailing surface nucleation. ^{31}P MAS NMR spectra of the 2 glasses showed the same shape and almost same width, which reflects a similar local environment for P in these glasses. The position of the resonance for W-containing glass at a more negative chemical shift than the Mo-containing one is attributed to the larger electrical field strength of W atoms than Mo atoms. ^{31}P MAS NMR spectra of crystals revealed two resonances at +17 and -0.5 ppm for the Mo glass and at -0.1 and -1.9 ppm for the W glass, reflecting the presence of two different phosphorus short range environments, in agreement with their crystal structure. Raman spectra showed similarity in structural features for Mo and W glasses and isomorphic compounds. Splitting of the dominant Raman bands in the crystal spectra reflects a distortion of MoO_6 and WO_6 octahedra. Raman spectra also suggested the breaking of Mo-O-Mo and W-O-W linkages during crystallization.

Introduction

WO_3 and MoO_3 are two transition metal oxides, which form glasses with phosphorus pentoxide P_2O_5 over a wide range of composition [1-4]. In these glasses MoO_3 and WO_3 easily change their valence state from W^{6+} and Mo^{6+} to W^{5+} and Mo^{5+}, respectively, so that both states are present in the glasses. Such glasses reveal interesting electrical properties due to the transfer of an unpaired d-electron of a transition metal ion in a lower oxidation state (Me^{5+}) to the upper oxidation state (Me^{6+})[5,6].

Study of crystallization of various ternary glasses with MoO_3 or WO_3 revealed that in several ternary systems a crystalline compound is formed at the $25MO(M_2O)$-$50MoO_3(WO_3)$-$25P_2O_5$ composition. In the ternary system PbO-MoO_3-P_2O_5, Masse et al. [7] prepared such a compound by the reaction of lead tetraphosphate with molybdenum oxide at 650°C and described its composition as $Pb(MoO_2)_2(PO_4)_2$. From XRD analysis of single crystals, they solved its structure consisting of chains of inter-connected PO_4 tetrahedra and MoO_6 octahedra linked via Mo-O-P bridges between their corners [7]. We have prepared this compound by crystallization of the glass composition 25PbO-$50MoO_3$-$25P_2O_5$ [8] and studied glass to crystal transformation at this glass composition [9]. Santagneli et al. studied glass to crystal transformation in the $AgPO_3$-MoO_3 glasses, where similar compound of the composition of $AgMoO_2PO_4$ was described [10,11].

During the study of the PbO-WO_3-P_2O_5 glasses, we have observed that crystallization of the glass composition 25PbO-$50WO_3$-$25P_2O_5$ produces a new crystalline compound with XRD data similar to that in the ternary system with molybdenum, i.e. $Pb(WO_2)_2(PO_4)_2$ [12] We were able to determine only the parameters of its elementary cell and its melting point [12]. In the BaO-MoO_3-P_2O_5 ternary system, Masse et al. [7] described the formation of a similar compound. We have observed during the crystallization of 25BaO-$50MoO_3$-$25P_2O_5$ glass the formation of a crystalline compound [13], but its diffraction pattern and unit cell parameters were different from the data given by Masse et al. [7]. Considering the complexity of lead and barium containing compositions, we decided to investigate the equivalent sodium composition for which more crystallographic data are available.

We have investigated structure and properties of sodium molybdato-phosphate glasses $40Na_2O$-$xMoO_3$-$(60-x)P_2O_5$ and compared them with similar sodium tungstato-phosphate glasses $40Na_2O$-yWO_3-$(60-y)P_2O_5$ with 1D ^{31}P MAS NMR spectroscopy and Raman spectroscopy [14]. Moreover we were able to prepare glasses within the broad concentration range of x(y) = 0-50 mol% of the modifying oxides MoO_3 and WO_3, respectively. We have

found in literature [15] that in these ternary systems similar compounds $NaMoO_2PO_4$ and $NaWO_2PO_4$ were prepared by the reaction of oxides WO_3 or MoO_3 with $NaPO_3$ and their structure was studied by Kierkegaard in 1961 [15].

Several papers were published dealing with glasses of the Na_2O-MoO_3-P_2O_5 system. Glass-forming region in this ternary system was determined in [16], but it is in an unusual form Na_2O-$(MoO_3)_2$-P_2O_5 and thus the glass-forming region looks smaller due to a double content of MoO_3 in the diagram. The authors [16] devoted their effort namely to the study of electrical conductivity of these glasses in three different compositional series corresponding to either a fixed Na_2O content or a constant Mo/P ratio.

Glasses in the compositional series $NaPO_3$-MoO_3 were studied by Bih et al. [17] and Santagnelli et al. [18]. Whereas the authors [17] applied only FTIR, DSC and EPR technique for their study of glasses within the concentration span of 0-50 mol% MoO_3, in [18] advanced NMR techniques and Raman spectroscopy were used for glasses containing 0-70 mol% MoO_3. Structural studies of $NaPO_3$-WO_3 glasses with advanced NMR techniques and Raman spectroscopy were also reported by de Araujo [19] As no report on the crystallization of the Na_2O-$MoO_3(WO_3)$-P_2O_5 glasses exists, we propose in the present study to complete the above mentioned data by the investigation of glass to crystal transformation of $25Na_2O$-$50MoO_3$-$25P_2O_5$ and $25Na_2O$-$50WO_3$-$25P_2O_5$ glasses.

Experimental

Glasses of the composition $25PbO.50MoO_3.25P_2O_5$ and $25PbO$-$50WO_3$-$25P_2O_5$ were prepared by melting Na_2CO_3 (99%; Penta), MoO_3 (99.5; Sigma-Aldrich), WO_3 (99.9; Fluka Analytical), and H_3PO_4 (85 wt%, p.a. Sigma-Aldrich) using a total batch weight of 30 g. The homogenized starting mixtures were slowly calcined up to 600°C with the final calcination at the maximum temperature for 2 hrs in order to remove the water. The reaction mixtures were then melted at 900-1000°C under ambient air, in a platinum crucible. The melt was subsequently poured into a preheated graphite mould ($T<T_g$) and the obtained glass was then cooled to room temperature. The weight of the glass sample together with the remaining melt in the crucible was usually more than 98 wt% and thus the weight loss was usually less than 2 wt%. This is why we assume that the glass compositions are not significantly different from the expected nominal composition, and will be considered as such in the following. The amorphous character of the prepared glasses was checked by X-ray diffraction analysis.

The glass density, ρ, was determined with bulk samples with the Archimedes method

using toluene as the immersion liquid. The molar volume, V_M, was calculated using the expression:

$$V_M = \bar{M}/\rho,$$

where $\bar{M}$ is the average molar weight of the glass composition a.M(Na_2O) + b.M(MoO_3/WO_3) + c.M(P_2O_5) calculated for $a+b+c = 1$. Density of polycrystalline samples was determined using a helium gas pycnometer AccuPyc II 1340, whereby the volume of the sample was measured by measuring the volume of the helium gas displaced by the sample. Molar volume was then calculated from the equation above.

The chemical durability of the glasses was evaluated from the measurement of the dissolution rate, DR, at 25 °C on glass cubes with a dimension of ~5 x 5 x 5 mm. The glass cubes were shaken in 100 cm^3 of distilled water for 24 h. The dissolution rate was calculated from the expression:

$$DR = \Delta\omega/St,$$

where $\Delta\omega$ is the weight loss (g), S is the sample area (cm^2) before the dissolution test and t is the dissolution time (min).

The thermal behaviour of the glasses was studied with a DTA 404 PC (Netzsch) operating in the DSC mode at a heating rate of 10 °C min^{-1} over the temperature interval 30-1000°C. The measurements were carried out with 60 mg powder samples (average particle size was 10 μm) in a silica crucible in an inert N_2 atmosphere. The thermal expansion coefficient, α, the glass transition temperature, T_g, and the dilatometric softening temperature, T_d, were measured using a dilatometer DIL 402 PC (Netzsch). Bulk samples, with dimensions of 20×5×5 mm^3, were cut out from larger piece with a diamond saw. From the obtained dilatometric curves, the coefficient of thermal expansion, α, was determined as the mean value in the temperature range of 150–250°C. The glass transition temperature, T_g, was determined from the change in the slope of the elongation vs. temperature plot and dilatometric softening temperature, T_d, was determined as the maximum of the expansion trace corresponding to the onset of viscous deformation. The dilatometric measurements were carried out in air at a heating rate of 5°C min^{-1}.

IR spectra were recorded at spectral resolution of 2 cm^{-1} using a Nicolet Protege 460 FT-IR spectrometer in the 400-4000 cm^{-1} range, with 32 scans. Powdered samples were mixed and homogenized with spectroscopically pure KBr and pressed into pellets.

Raman spectra in the range 1400-200 cm^{-1} were measured on bulk and powder samples at room temperature using a DXR Raman spectrometer Thermo Scientific DXR SmartRaman with a 532 nm solid state (Nd:YAG) diode pumped laser.

^{31}P MAS NMR spectra were measured at 9.4 T on a BRUKER Avance 400 spectrometer with a 4 mm probe. The spinning speed was 12.5 kHz and relaxation (recycling) delay was 180s. The chemical shifts of ^{31}P nuclei are given relative to H_3PO_4 at 0 ppm.

A Bruker D8 Advance diffractometer and $Cu_{K\alpha}$ radiation was used for the study of annealed glass powders. A database of inorganic compounds from the International Center of Diffraction Data [20] was used for the phase identification.

Results and discussion

For the study of glass to crystal transformation we have prepared $25Na_2O.50MoO_3.25P_2O_5$ and $25Na_2O.50WO_3.25P_2O_5$ glasses by the procedure described above. Both glassy samples were of dark blue color due to the presence of Mo^{5+} and W^{5+} ions, respectively, in the prepared glasses. The values of the density and molar volume of both glasses are given in Table 1.

Thermal behaviour of both glasses was studied by differential thermal analysis and dilatometry. The curves from DTA measurements are shown in Fig. 1. On the obtained DTA curves we can see exothermic crystallization peaks and sharp endothermic melting peaks. Both curves reveal also a small step before the crystallization peak corresponding to the change of c_p in the glass transformation region. Glass transition temperature, determined from DTA curves, is 403°C for the $25Na_2O.50MoO_3.25P_2O_5$ glass and 505°C for the $25Na_2O.50WO_3.25P_2O_5$ glass. Sharp crystallization peaks are typical of the formation of a single crystalline compound in both glasses. Their position depends on the size of analyzed glass powder. In Fig. 1a. glass samples milled to the size of 8-10 um were used, whereas in Fig. 1b three bulk pieces were used for the DTA measurement. For the fine glass powder with molybdenum, the onset of crystallization peak is 487°C, whereas for the bulk pieces is 532°C. For the fine glass powder with tungsten, the onset of crystallization peak is 624°C, whereas for the bulk pieces is 688°C. This behavior is typical of a surface nucleation mechanism, but it will be further studied in the following. As can be seen in Fig.1, melting peak remains as expected on the same place for fine and bulk samples and the melting temperature of the sample with tungsten is 875°C, whereas for the sample with molybdenum it is 712°C.

The values of thermal expansion coefficient, α, are of both glass samples are given in Table 2 (the curves are not shown). For the $25Na_2O.50MoO_3.25P_2O_5$ glass we have obtained the value of $\alpha = 14.1\pm0.3$ ppm $°C^{-1}$ and slightly lower value of of $\alpha = 13.7\pm0.3$ ppm $°C^{-1}$ was obtained for the $25Na_2O.50WO_3.25P_2O_5$ glass.

Larger difference between these two glasses were obtained for the dissolution rate, DR, The $25Na_2O.50WO_3.25P_2O_5$ glass, which has DR = $0.5x10^{-5}$ g cm^{-2} min^{-1}, is much more durable than $25Na_2O.50MoO_3.25P_2O_5$ glass with DR = 10.1 $x10^{-5}$ g cm^{-2} min^{-1}.

We have used the data obtained from DTA measurements for the choice of heat-treatment temperature for fine powder glass samples to crystalize them. In both cases we annealed the samples above crystallization peak observed in Fig. 1a, i.e. at 550°C for the $25Na_2O.50MoO_3.25P_2O_5$ glass and at 700°C for the $25Na_2O.50WO_3.25P_2O_5$ glass. In both cases, the temperature was held for 2 hr and after cooling the crystallized samples to the room temperature, X-ray diffraction was applied for the analysis of both products.

X-ray diffraction lines (Fig. 2) were in a good agreement with the X-ray diffraction diagrams of the $NaMoO_2PO_4$ and $NaWO_2PO_4$ compounds [15], and no other crystalline phase was detected.

We have determined the density of the obtained polycrystalline samples with the helium gas pycnometer and found the values of 3.57 g cm^{-3} for the compound $NaMoO_2PO_4$ (glass density 3.31 g cm^{-3}) and 4.91 g cm^{-3} for the compound $NaWO_2PO_4$ (glass density 4.53 g cm^{-3}). Higher values of density of crystalline samples in comparison with corresponding glasses and lower values of the molar volume of the polycrystalline samples in comparison with corresponding glasses (Table 1) are in agreement with the theoretical volume-temperature diagram for glass-forming liquids [21].

For the glass compositions $25Na_2O.50MoO_3.25P_2O_5$ and $25Na_2O.50WO_3.25P_2O_5$, differential thermal analysis was used for the study of the dominant crystallization mechanism by the method of Ray and Day [22]. The crystallization mechanism (surface or internal nucleation) was evaluated from changes in the shape and position of the crystallization peak on DTA curves with the particle size (120, 300, 600 and 900 μm) of the studied glasses. As can be seen on Fig.3, the shape of the crystallization peak changes substantially with changes in the particle size of the glass. When increasing the grain size of the sample, the crystallization peak shifts to higher temperatures and its height decreases, while the width of the peak increases. This behavior, according to [22], is typical for the surface crystallization. These results suggest that the glasses of the composition $25Na_2O.50MoO_3.25P_2O_5$ and $25Na_2O.50WO_3.25P_2O_5$ nucleate predominantly via the surface crystallization mechanism, thereby producing crystalline compound $NaMoO_2PO_4$ and $NaWO_2PO_4$, respectively.

Optical microscopy confirmed the mechanism of surface crystallization. We have observed that crystallization starts from the surface and continues to the core of the glass sample. In Fig. 4 there is a picture from the optical microscope showing inside dark glass phase and outside

clear crystalline phase of the sample $25NaO.50MoO_3.25P_2O_5$ annealed at 570°C for 4 hr. We have to use higher tempeture for annealing bulk sample to be able to observe crystallization procedure. Simulaneously with crystallization process oxidation of Mo^{5+} to Mo^{6+} took place and the blue colour of the glass changed to a slightly yellow crystalline phase. Similar decolorization of the sample we observed at the annealing of the $25PbO.50WO_3.25P_2O_5$ glasses.

Raman spectra of $25NaO.50MoO_3.25P_2O_5$ and $25PbO.50WO_3.25P_2O_5$ glasses and its crystalline counterparts $NaMoO_2PO_4$ and $NaWO_2PO_4$, respectively, are shown in Fig 5. Raman spectrum of the $25NaO.50MoO_3.25P_2O_5$ glass (Fig 5a) is in a good agreement with that obtained by Santagneli et al. [18] in their studies of $NaPO_3$-MoO_3 glasses. Similarly, the Raman spectrum of the $25NaO.50WO_3.25P_2O_5$ glass is in a good agreement with that obtained by de Araujo et al. [19] in their studies of $NaPO_3$-WO_3 glasses. The dominant bands at 958 cm^{-1} in the Mo-containing glass and at 961 cm^{-1} in the W-containing glass are assigned to vibrations of terminal molybdenum-oxygen bonds in the molybdate polyhedra and tungstate polyhedra, respectively [18,19]. The medium band at 840 cm^{-1} in the $25NaO.50MoO_3.25P_2O_5$ glass was ascribed to the stretching vibrations of Mo-O-Mo bonds [18]. In the Raman spectrum of the $25NaO.50WO_3.25P_2O_5$ glass (Fig. 5b) the medium vibrational band at 837 cm^{-1} seems to be broader and with higher amplitude than the corresponding band in the Mo-containing glass and we ascribe it also to the vibrations of single W-O bonds in the W-O-W bridges, in agreement with [19]. From this comparison it seems that clustering of tungsten polyhedra is higher than the clustering of molybdate polyhedra.

Raman spectra of polycrystalline samples of $NaMoO_2PO_4$ and $NaWO_2PO_4$ are also shown in Fig. 5. Raman spectra of both polycrystalline compounds reveal similar features due to the similar structure of both compounds. Instead of the dominant peak of vibrations of $W\text{-}O^-$ bonds there are three bands 927, 899 and 876 cm^{-1} at the $NaMoO_2PO_4$ polycrystalline sample (Fig. 5a) and 946, 905 and 887 cm^{-1} at the $NaWO_2PO_4$ polycrystalline sample (Fig. 5b). Splitting of the main bands in both compounds is due to the distortion of MoO_6 and WO_6 octahedra in both compounds [24]. In Fig. 6 is shown the short range environment of the Mo atoms in $NaMoO_2PO_4$ compound [15] and W atoms in the $NaWO_2PO_4$ compound [15]. Both compounds are isostructural and in both compounds Mo and W atoms are bonded by four bonds to phosphorus atoms and by two bonds to terminal oxygen atoms. Terminal P-O bonds are shorter than Mo-O-P and W-O-P bonds, which results in the existence of distorted MoO_6 and WO_6 octahedra and splitting of the Raman bands ascribed to ν_1 vibrations of MoO_6 and WO_6 octahedra. Similar splitting was observed also in the Raman spectra of $Pb(MoO_2)(PO_4)$ and $Ba(MoO_2)(PO_4)$ compounds [25].

Close positions of the dominant vibrational bands both in the glass and in the crystal support the idea that the coordination of Mo and W atoms does not change at crystallization, i.e. MoO_6 and WO_6 octahedra exist also in $25NaO.50MoO_3.25P_2O_5$ and $25PbO.50WO_3.25P_2O_5$ glasses, respectively. Crystallization of these glasses destroys Mo-O-Mo and W-O-W linkages, because in crystalline compounds there are only four Mo-O-P and Mo-O-W bonds on each octahedron and two terminal bonds Mo-O or W-O. This difference is reflected in the Raman spectra of crystalline compounds by the absence of the broad band in the region of 700-850 cm^{-1} present on the Raman spectra of glasses.

Infrared spectra of $25NaO.50MoO_3.25P_2O_5$ and $25PbO.50WO_3.25P_2O_5$ glasses and its crystalline counterparts $NaMoO_2PO_4$ and $NaWO_2PO_4$, respectively, are shown in Fig 7. Infrared spectrum of the $25NaO.50MoO_3.25P_2O_5$ glass is similar to that obtained by Santagnelli et al. [18] and by Bih et al. [17] in their study of $NaPO_3$-MoO_3 glasses. The IR spectrum shown in Fig.6 reveals absorption bands at 1180, 941, 906, 752, 640 and 542 cm^{-1}. The authors [18] in their description of IR spectra mention only the band at ~1200 cm^{-1}, which were assigned to terminal P-O bond stretching vibration. The most intense absorption bands at ~906 cm^{-1} and 941 cm^{-1} are ascribed to the vibration of Mo-O bonds in MoO_6 octahedra [17, 26]. The absorption band of 906 cm^{-1} is assigned to the vibration of ν_{as} (P-O-Mo) bonds and that at 941 cm^{-1} to ν_{as}(Mo=O) vibration [17]. The absorption band at 752 cm^{-1} is ascribed to ν_s(P-O-Mo) and the band at 640 cm^{-1} is ascribed to ν_s (Mo-O-Mo) [17]. The absorption band at 542 cm^{-1} belongs to bending vibrations of phosphate groups [17]. Infrared spectrum of $25PbO.50WO_3.25P_2O_5$ glass is similar to the spectrum of the Mo-containing glass and its assignment would be also similar.

Infrared spectra of crystalline compounds $NaMoO_2PO_4$ and $NaWO_2PO_4$ are also very similar (Fig. 7) due to their similar structures. There are two groups of strong absorption bands at 850-950 cm^{-1} and at 950-1100 cm^{-1}. When we apply the results of analysis of the IR spectra of the compounds $Pb(MoO_2)_2(PO_4)_2$ and $Ba(WO_2)_2(PO_4)_2$ [25], we can assign the first group of absorption bands to vibrations of Mo-O bonds in MoO_6 octahedra, whereas the second group contains absorption bands of phosphate groups [17, 27]. Bands with medium amplitude at 450 cm^{-1} can be assigned to infrared active ν_4 vibration of MoO_6 octahedra [17]. The assignment of bands in the infrared spectra of the polycrystalline $NaWO_2PO_4$ will be similar to the spectra of $NaMoO_2PO_4$.

^{31}P MAS NMR spectra of $25Na_2O$-$50MoO_3$-$25P_2O_5$ and $25Na_2O$-$50WO_3$-$25P_2O_5$ glasses are shown in Fig. 8. These two spectra have same shape and almost the same width,

which reflects a similar local environment for phosphorus in these glasses. Both spectra contain one broad resonance, which is centered on -4.4 ppm for the Mo-containing glass and -7.0 ppm for the W-containing glass. The difference in chemical shift is not so large, but it may reflects some difference in the local structure around the PO_4 groups in the glasses. First, we can consider the O/P ratio, which gives a rough estimation of the phosphate polymerization [28]. It is 3 for metaphosphate groups (i.e. chains, or Q^2 groups), 3.5 for pyrophosphate groups (dimeric units or chain-end groups, Q^1) and 4 for orthophosphates (isolated PO_4 groups, Q^0). The O/P ratio is 6 for both glasses and since it is larger than 4, it means that on average all the phosphate units are not connected to each other, and the excess of oxygens belong to molybdate or tungstate groups (which are probably MoO_6 and WO_6, respectively [8,10,19]) Hence, we can assume that in both glasses only Q^0 sites are present, meaning that the difference in the ^{31}P chemical shift is not due to a difference in the polymerization degree. We may then consider a second structural parameter that influences the ^{31}P chemical shift, which is the electrostatic field strength (EFS, Z/r^2, where Z is the ionic charge, r is ionic radius) of the second neighbor of phosphate groups (Na or Mo/W). A larger EFS induces a more negative ^{31}P chemical shift, as reported by Brow et al. [29]. Therefore we think that the shift to more negative value of W-containing glass is is due to the larger electrical field strength of W than Mo.

We have also recorded the ^{31}P MAS NMR spectra of polycrystalline $NaMoO_2PO_4$ and $NaWO_2PO_4$ compounds and their comparison with the spectra of the corresponding glasses is also shown in Fig. 8. The presence of two signals in both ^{31}P MAS spectra (at +1.7 and -0.5 ppm for $NaMoO_2PO_4$ and -0.1 and -1.9 ppm for $NaWO_2PO_4$) reveals two different phosphorus local environments in these compounds. Structural study of Kierkegaard [15] showed that these two compounds are isostructural, hence the local environment of phosphorus atoms is identical in both compounds. The coordination of phosphorus atoms according to [15] is shown in Fig.9. We can see that in $NaMoO_2PO_4$ there are two different phosphorus sites (marked as P1 and P2) charge compensated by Mo and Na. This is reflected by the presence of two resonances on the ^{31}P NMR spectra (Fig. 8). The difference in chemical shifts between the $NaMoO_2PO_4$ and $NaWO_2PO_4$ is, again, due to the EFS effect of molybdenum and tungsten. The height of both resonances should be identical, but the resonance at a higher chemical shift has a smaller amplitude because of its larger width. This reflects that the local environment of phosphorus is less symmetrical for the resonance at larger chemical shift (less negative value). Looking at the short range environment of phosphorus atoms (Fig. 9) indicates that this latter resonance can be assigned to P1 site, which has less symmetrical local environment, as reflected by larger differences in P-O bond lengths as compared to phosphorus sites P2. Moreover, phosphorus

atom P1 is charge compensated by 4 Mo and 2 Na atoms, whereas P2 is charge compensated by 4 Mo and 3Na atoms, which may explain why P2 resonance has a more negative shift value. The same interpretations holds for $NaWO_2PO_4$ since both structures are identical.

Conclusion

In this study we compared structure of two glasses $25Na_2O.50MoO_3.25P_2O_5$ and $25Na_2O.50MoO_3.25P_2O_5$ and their corresponding crystalline compounds. ^{31}P MAS NMR and Raman spectroscopy enabled to probe phosphorus and molybdenum environments in these glasses and corresponding $NaMoO_2PO_4$ and $NaWO_2PO_4$ crystals. ^{31}P MAS NMR reflected structural studies of Peder Kierkegaard from 1961 showing two different coordinations of phosphorus atoms in the $NaMoO_2PO_4$ and $NaWO_2PO_4$ crystals, but only one average site could is observed in the glasses of the same composition. Splitting of the main vibrational band of MoO_6 and WO_6 octahedra in the Raman spectra of crystalline compounds reflects the presence of distorted MoO6 and WO6 octahedra in crystalline compounds $NaMoO_2PO_4$ and $NaWO_2PO_4$. Our studies support octahedral coordination of molybdenum and tungsten in the studied glasses. Raman spectra show on the breaking of Mo-O-Mo and W-O-W linkages during glass crystallization.

Acknowledgements

The Czech authors are grateful for the financial support from the project No. 18-01976S of the Grant Agency of the Czech Republic. LM thanks the Chevreul Institute (FR 2638) for its help in the development of this work. Chevreul Institute is supported by the Ministère de l'Enseignement Supérieur et de la Recherche, the Région Nord-Pas de Calais and the Fonds Européen de Développement des Régions.

References

1. N.D Patel, B. Bridge, The effect of Mo^{5+} ions (in the presence of Mo^{6+} ions) on the elastic moduli of molybdenum phosphate glasses, Phys. Chem. Glasses 24 (1983) 130-134.

2. B. Bridge, N.D. Patel, Thermal analysis of molybdenum phosphate glasses between room temperature and the softening point, Phys. Chem. Glasses 27 (1986) 235-240.

3. B. Bridge, N.D. Patel , Composition dependence of the infra-red absorption spectra of molybdenum phosphate glasses and some crystalline analogues, J. Non-Cryst. Solids 91 (1987) 27-42.

4. S.H. Morgan, R.H. Magruder, Raman spectra of molybdenum phosphate glasses and some crystalline analogues, J. Am. Ceram. Soc 73 (1990) 753-756.

5. L, Bih, M. El Omari, J.M. Réau, A. Nadiri, A. Yacoubi, M. Haddad, Electrical properties of glasses in Na_2O-MoO_3-P_2O_5 system, Mater. Letters 50 (2001) 308-317.

6. D. Boudlich, L. Bih, M. Archidi. El H., M, Haddad, A. Yacoubi, A. Nadiri, B. Elouadi, Infrared, Raman, and Electron Spin Resonance Studies of Vitreous Alkaline Tungsten Phosphates and Related Glasses, J. Am. Ceram. Soc. 85 (2002) 623-630.

7. R. Masse, M.T. Averbuch-Pouchot, A. Durif, J. Solid State Chem. 58 (1985) 157-163.

8. L. Koudelka, I. Rösslerová, J. Holubová, P. Mošner, L. Montagne, B. Revel, Structural study of PbO-MoO_3-P_2O_5 glasses by Raman and NMR spectroscopy, J. Non-Cryst. Solids 357 (2011) 2816-2821.

9. I. Rösslerová, L. Koudelka, Z. Černošek, P. Mošner, L. Beneš, Thermal properties and crystallization of PbO-MoO_3-P_2O_5 glasses, J. Mater. Sci. 46 (2011) 6751-6757.

10. S.H. Santagneli, J. Ren, M.T. Rinke, S.J.L. Ribeiro, Y. Messaddeq, H. Eckert: Structural studies of $AgPO_3$-MoO_3 glasses using solid state NMR and vibrational spectroscopies, J. Non-Cryst. Solids 358 (2012) 985-992.

11. P. Kierkegaard, S. Holmen, The crystal structure of $AgMoO_2PO_4$, Ark. Kemi 23 (1965) 213-221.

12. I. Rösslerová, L. Koudelka, Z. Černošek, P. Mošner, L. Beneš, Study of crystallization of PbO-WO_3-P_2O_5 glasses by thermoanalytical and spectroscopic methods, J. Non-Cryst. Solids 384 (2014) 41-46.

13. P. Kalenda, L. Koudelka, P. Mošner, L. Beneš, Z. Černošek, Thermal properties and crystallization of BaO-MoO_3-P_2O_5 glasses, J. Therm. Anal. Calorim. (in print).

14. P. Mošner, O. Kupetska, L. Koudelka, Sodium phosphate glasses modified by MoO_3 and WO_3, Phys. Chem. Glasses, Eur. J. Glass Sci. Technol. (submitted).

15. P. Kierkegaard, The crystal structure of $NaMoO_2PO_4$ and $NaWO_2PO_4$, Arkiv Kemi, 18 (1961) 553-575.

16. L. Bih, A. Nadiri, J. Aride, Thermal study of $A_2O(MoO_3)_2$-P_2O_5 (A=Li, Na), J. Therm. Anal. Calorim. 68 (2002) 965-972.

17. L. Bih L., A. Nadiri, Y. El Amraoui, Investigation of the physico-chemical properties of $NaPO_3$-MoO_3 glasses, J. Phys. IV France 123 (2005) 165-169.

18. S.H. Santagneli, C.C. de Araujo, W. Strojek, H. Eckert, G. Poirier, S.J.L. Ribeiro, Y. Messaddeq, Structural Studies of $NaPO_3$-MoO_3 Glasses by Solid-state Nuclear Magnetic Resonance and Raman Spectroscopy, J. Phys. Chem. B 111 (2007) 10109-10117.

19. C.C. de Araujo, W. Strojek, L. Zhang, H. Eckert, G. Poirier, S.J.L. Ribeiro, Y. Messaddeq, Structural studies of $NaPO_3$-WO_3 glasses by solid state NMR and Raman spectroscopy, J. Mater. Chem. 16 (2006) 3277-3284.

20. Joint Committee on powder diffraction standards, Swarthmore, PA, USA. International Centre of Diffraction Data.

21. A.K. Varshneya, Fundamentals of Inorganic glasses, 2nd edition, The Society of Glass Technology, Sheffield 2006, p. 19.

22. C.S. Ray, D.E. Day, Identifying internal and surface crystallization by differential thermal analysis for the glass-to-crystal transformations. Thermochim. Acta. 280-281 (1996) 163-174.

23. L. Koudelka, P. Kalenda, J. Holubová, P. Mošner, L. Montagne, B. Revel, Structural study of BaO-MoO_3-P_2O_5 glasses by Raman and NMR spectroscopy, J. Non-Cryst Solids 476 (2017) 114-121.

24. F.D. Hardcastle, I.E. Wachs, Determination of molybdenum-oxygen bond distances and bond orders by Raman spectroscopy, J. Raman Spectrosc. 21 (1990) 683-691.

25. M. Isaac, V. Jayasree, G. Suresh, V.U. Nayar, Vibrational spectra of $M(MoO_2)(PO_4)_2$ [M=Pb,Ba], Indian J. Phys. 66B (1992) 65-69.

26. L. Bih, A. Nadiri, M. El Omari, A. Yacoubi, M. Haddad, FTIR, EPR and x-ray investigation of mixed valence molybdenum phosphate A_2O-(MoO_3)-P_2O_5 (A=Li,Na) glasses, Phys. Chem. Glasses 43 (2002) 153-157.

27. C.E. Varsamis, E.I. Kamitsos, T., Minami, N. Machida, Investigation of CuI- containing molybdophosphate glasses by infrared reflectance spectroscopy, J. Phys. Chem. C 116 (2012) 11671-11681.

28. R.K. Brow, Review: the structure of simple phosphate glasses J. Non-Cryst. Solids 263-264 (2000) 1-28.

29. R.K. Brow, C.C. Phifer, G.L. Turner, R. J. Kirkpatrick, Cation effects on ^{31}P MAS NMR chemical shifts of metaphosphate glasses, J. Am. Ceram. Soc. 74 (1991) 1287-1290.

Figure captions

Fig. 1. DSC curves of $25Na_2O.50MoO_3.25P_2O_5$ glass and $25Na_2O.50WO_3.25P_2O_5$ glass for (a) fine glass powder and(b) for bulk pieces.

Fig. 2. XRD patterns of $NaMoO_2PO_4$ and $NaWO_2PO_4$ polycrystalline compounds obtained by annealing of fine powders of $25Na_2O.50MoO_3.25P_2O_5$ and $25Na_2O.50WO_3.25P_2O_5$ glasses, respectively.

Fig. 3. Crystallization peaks for (a) $25Na_2O.50MoO_3.25P_2O_5$ glass and (b) $25Na_2O.50WO_3.25P_2O_5$ glass, for different grain size of the sample. Note that the temperature scales are different.

Fig. 4. Microscopic picture of the crystallization procedure in the $25Na_2O.50MoO_3.25P_2O_5$ glass, showing cross-section of the glass partially annealed at 570°C for 4 hr. Dark core is the glassy phase and light cladding is the crystalline phase $NaMoO_2PO_4$.

Fig. 5. Raman spectra of (a) $25Na_2O.50MoO_3.25P_2O_5$ glass and the corresponding polycrystalline compound $NaMoO_2PO_4$ and (b) $25Na_2O.50WO_3.25P_2O_5$ glass and the corresponding polycrystalline compound $NaWO_2PO_4$.

Fig. 6. Short range environment of (a) the Mo atoms in the $NaMoO_2PO_4$ compound and(b) W atoms in the $NaWO_2PO_4$ compound according to the data of Kierkegard in Ref. [15].

Fig. 7. IR spectra of (a) $25Na_2O.50MoO_3.25P_2O_5$ glass and the corresponding polycrystalline compound $NaMoO_2PO_4$ and (b) $25Na_2O.50WO_3.25P_2O_5$ glass and the corresponding polycrystalline compound $NaWO_2PO_4$.

Fig. 8. ^{31}P MAS NMR spectra of (a) $25Na_2O.50MoO_3.25P_2O_5$ glass and the corresponding polycrystalline compound $NaMoO_2PO_4$ and (b) $25Na_2O.50WO_3.25P_2O_5$ glass and the corresponding polycrystalline compound $NaWO_2PO_4$.

Fig. 9. Short range environment of the P atoms in the $NaMoO_2PO_4$ crystalline compound according to the data of Kierkegaard in Ref. [15].

Table 1. Composition, density, ρ, and molar volume, V_M, of $25Na_2O.50MoO_3.25P_2O_5$ and $25Na_2O.50WO_3.25P_2O_5$ glasses and $NaMoO_2PO_4$ and $NaWO_2PO_4$ crystals .

Sample	Na_2O	MoO_3/WO_3	P_2O_5	ρ±0.02	V_m±0.5
	mol %			[g cm^{-3}]	[cm^3 mol^{-1}]
$25Na_2O-50MoO_3-25P_2O_5$	25	50	25	3.31	37.1
$NaMoO_2PO_4$	25	50	25	3.57	34.4
$25Na_2O-50WO_3-25P_2O_5$	25	50	25	4.53	36.9
$NaWO_2PO_4$	25	50	25	4.91	34.0

Table 2: Glass transition temperature T_g, dilatometric softening temperature T_d, thermal expansion coefficient, α and dissolution rate, DR, of $25Na_2O.50MoO_3.25P_2O_5$ and $25Na_2O.50WO_3.25P_2O_5$ glasses.

Sample	T_g±2	T_d±2	α±0.3 (150-250°C)	DR 10^5 ±0,2
	[°C]		[ppm $°C^{-1}$]	[g cm^{-2} min^{-1}]
$25Na_2O-50MoO_3-25P_2O_5$	410	427	14.1	10.1
$25Na_2O-50WO3-25P_2O_5$	505	537	13.7	0.5

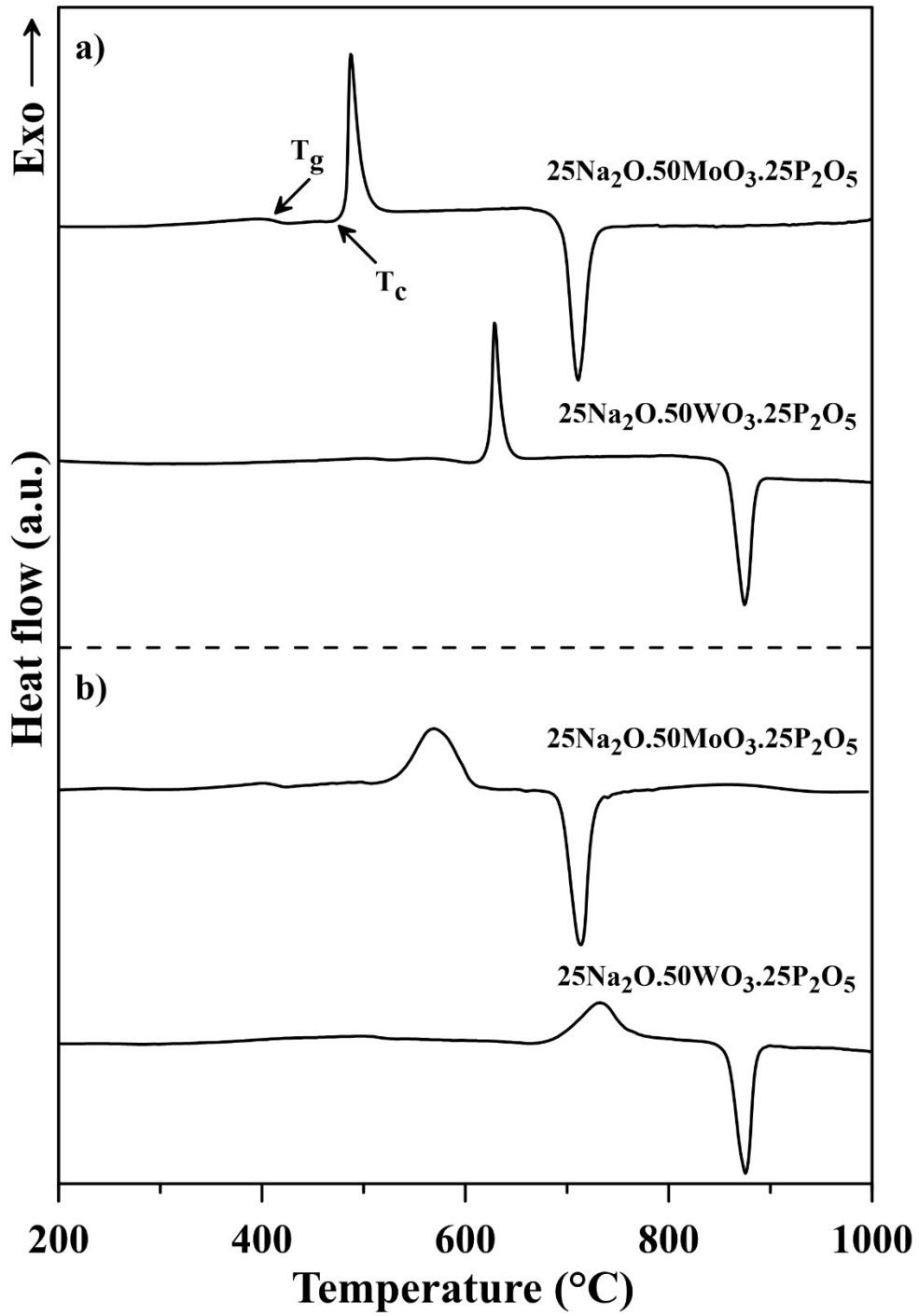

Fig. 1. DTA curves of $25Na_2O.50MoO_3.25P_2O_5$ glass and $25Na_2O.50WO_3.25P_2O_5$ glass for fine glass powder (a) and bulk pieces (b).

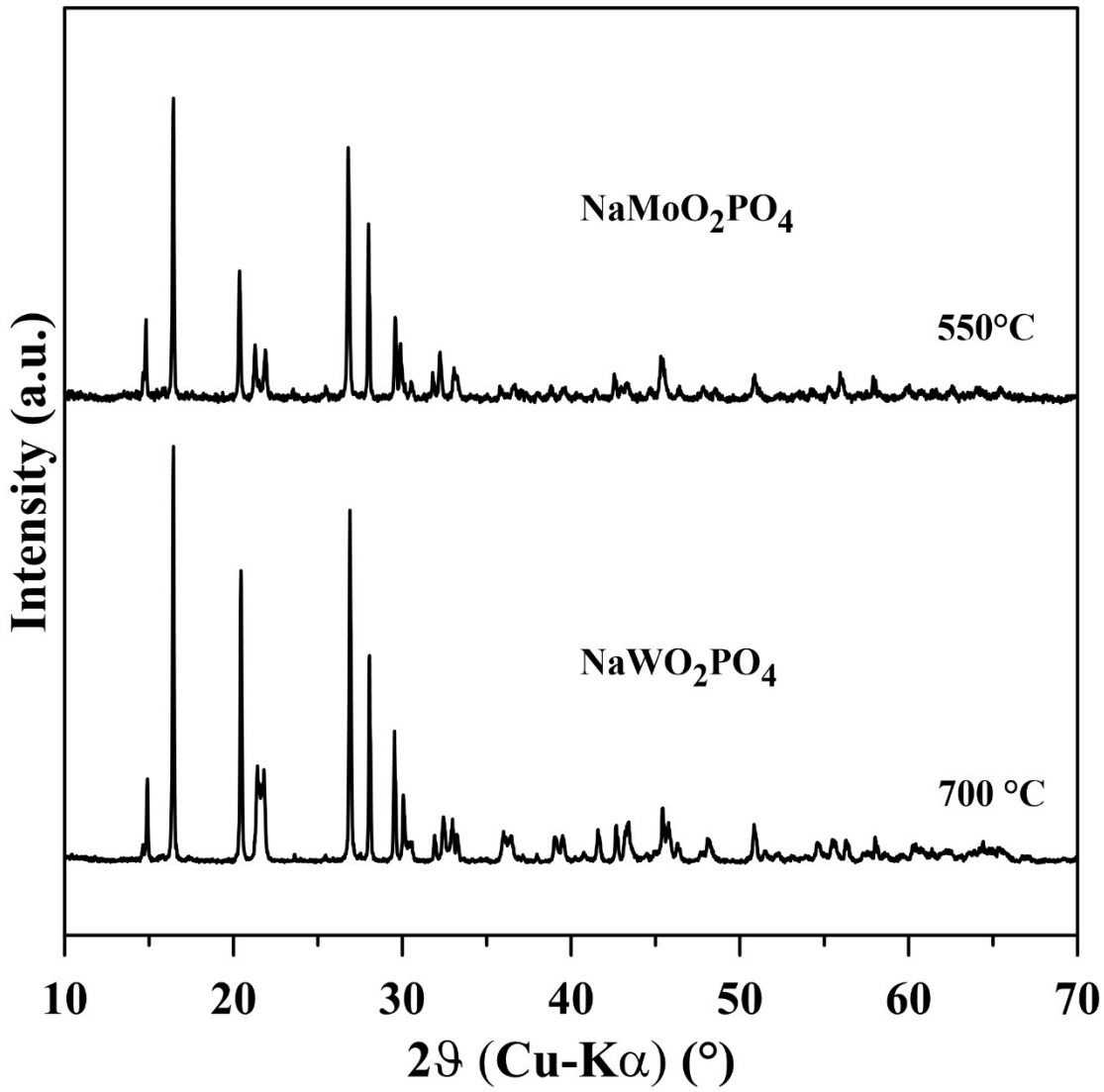

Fig. 2. XRD patterns of $NaMoO_2PO_4$ and $NaWO_2PO_4$ polycrystalline compounds obtained by annealing fine powders of $25Na_2O.50MoO_3.25P_2O_5$ and $25Na_2O.50WO_3.25P_2O_5$ glasses, respectively.

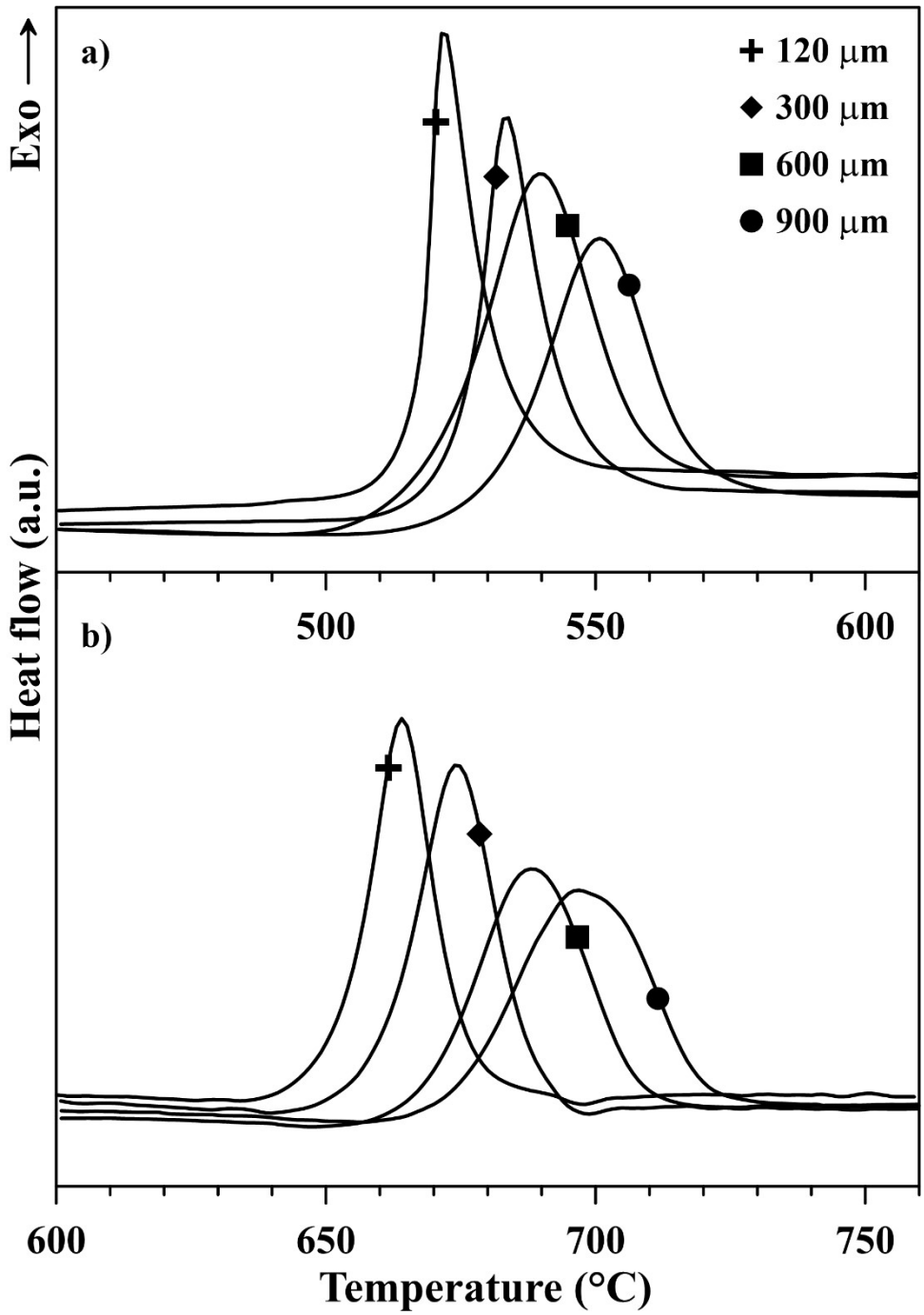

Fig. 3. The change of the crystallization peaks for $25Na_2O.50MoO_3.25P_2O_5$ glass (a) and $25Na_2O.50WO_3.25P_2O_5$ glass (b) depending on the grain size of the sample.

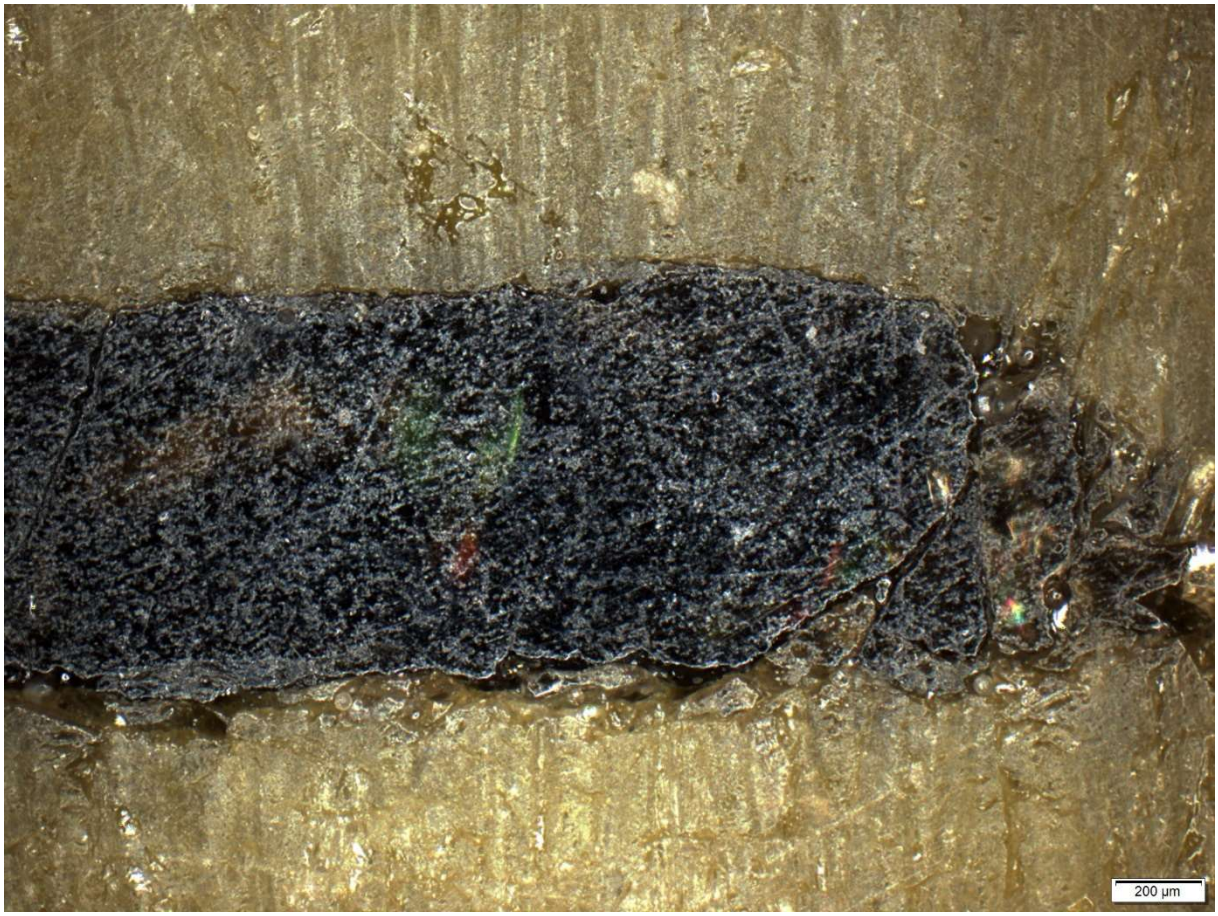

Fig. 4. Microscopic picture of the crystallization procedure in the $25Na_2O.50MoO_3.25P_2O_5$ glass, showing cross-section of the glass partially annealed at 570°C for 4 hr. Dark core is the glassy phase and light cladding is the crystalline phase $NaMoO_2PO_4$.

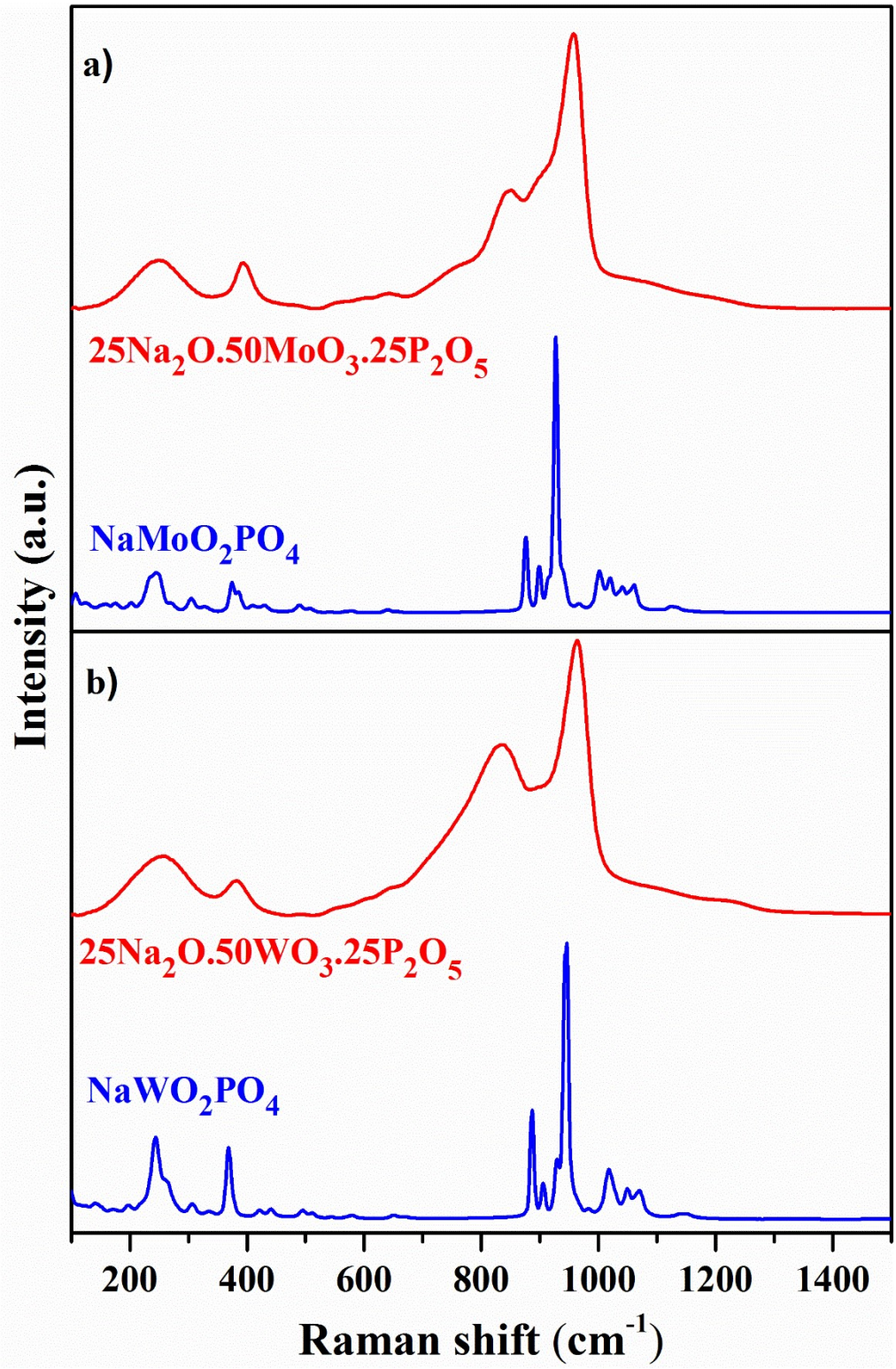

Fig.5. Raman spectra of $25Na_2O.50MoO_3.25P_2O_5$ glass and the corresponding polycrystalline compound $NaMoO_2PO_4$ (a) and $25Na_2O.50WO_3.25P_2O_5$ glass and the corresponding polycrystalline compound $NaWO_2PO_4$ (b).

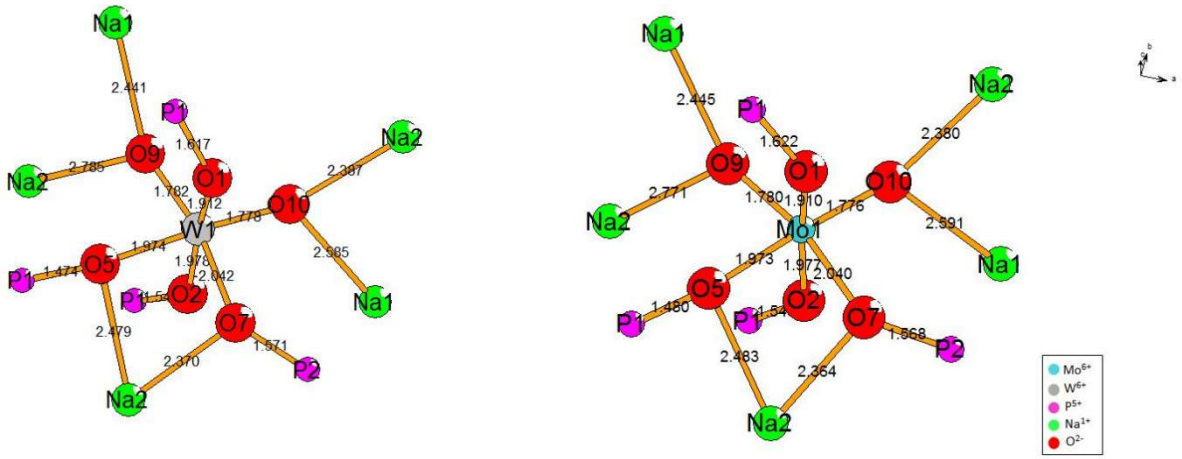

Fig. 6. Short range environment of the Mo atoms in the $NaMoO_2PO_4$ compound (b) and W atoms in the $NaWO_2PO_4$ compound (a) according to the data of Kierkegard in Ref. [15].

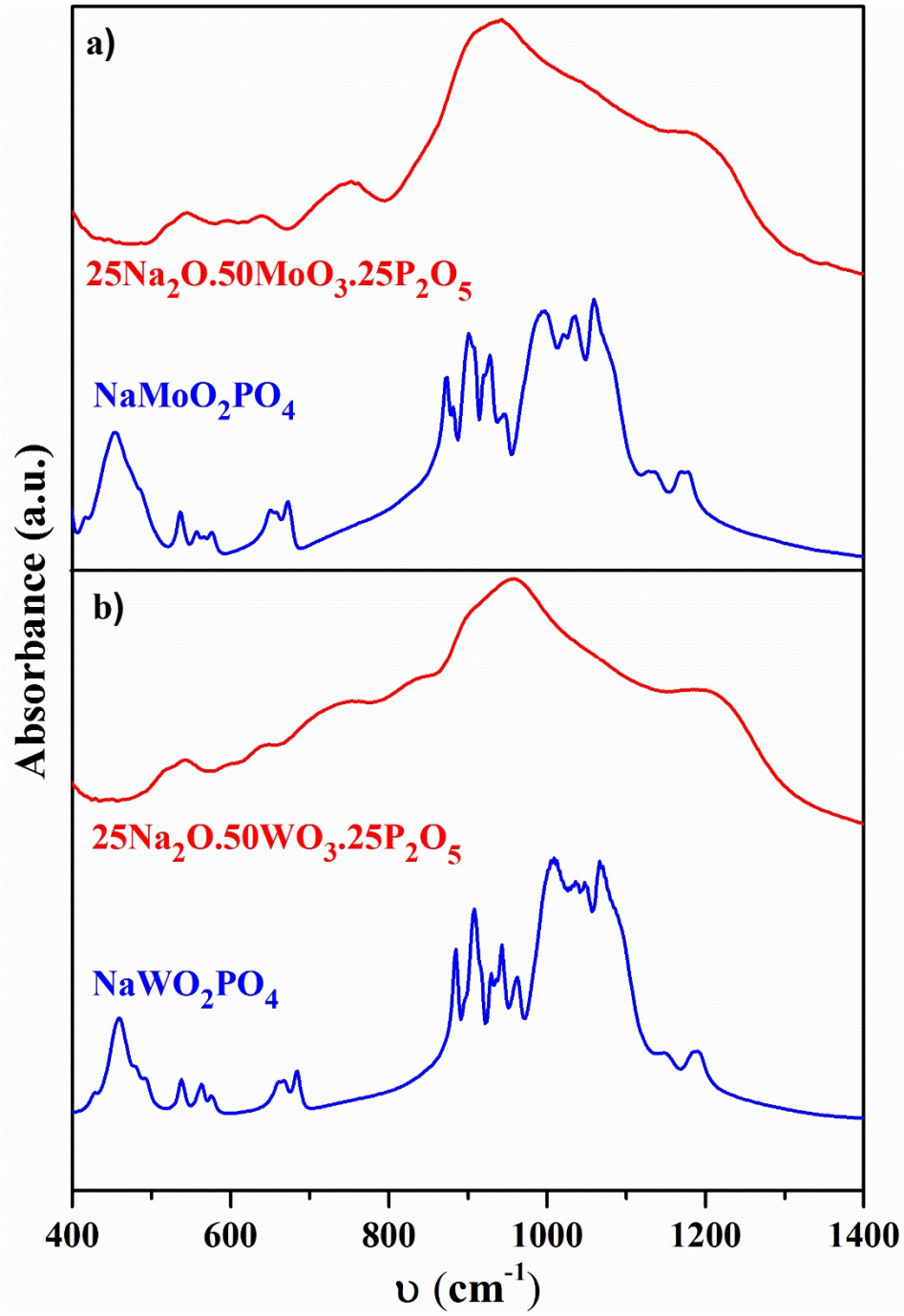

Fig. 7. IR spectra of $25Na_2O.50MoO_3.25P_2O_5$ glass and the corresponding polycrystalline compound $NaMoO_2PO_4$ (a) and $25Na_2O.50WO_3.25P_2O_5$ glass and the corresponding polycrystalline compound $NaWO_2PO_4$ (b).

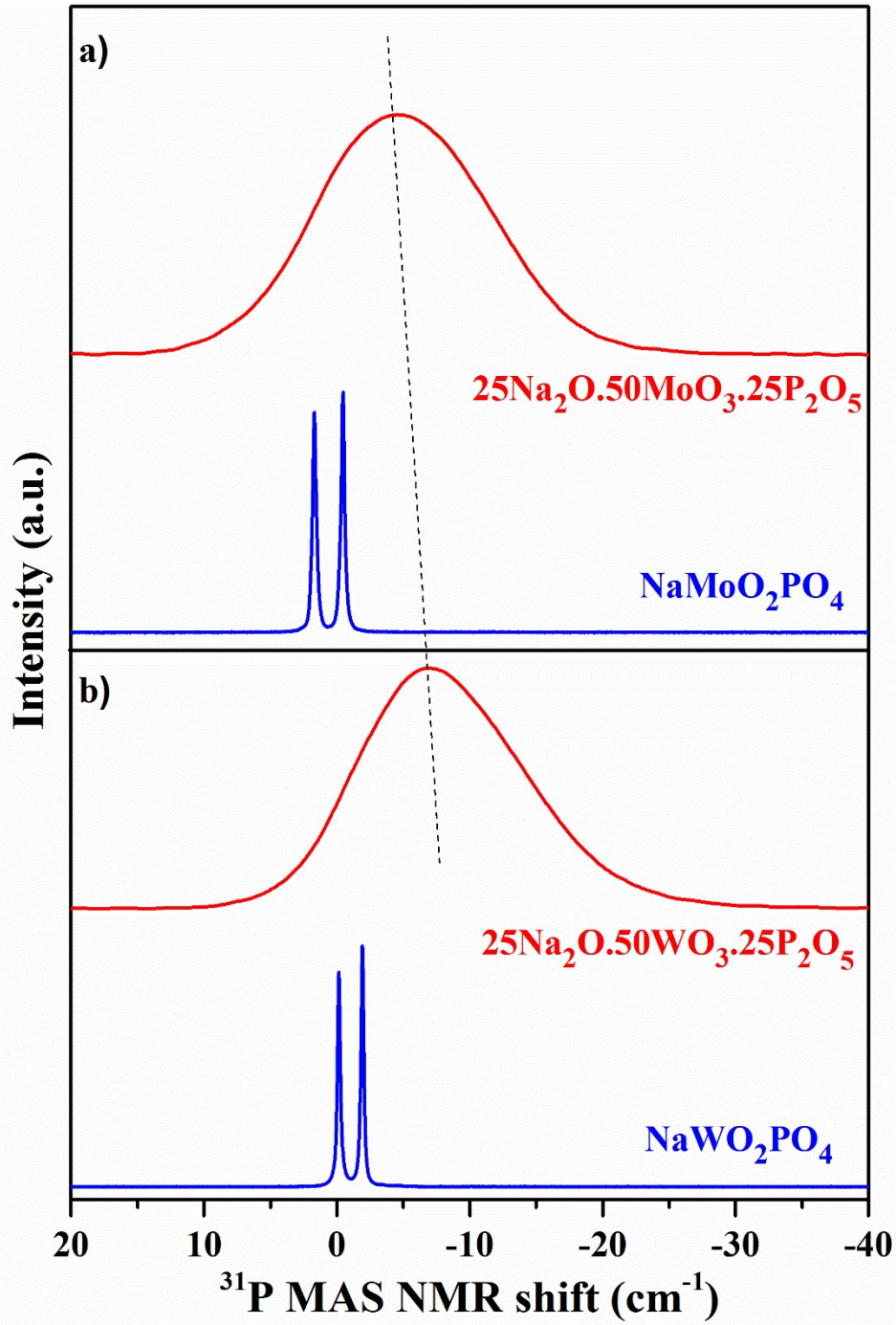

Fig. 8. ^{31}P MAS NMR spectra of $25Na_2O.50MoO_3.25P_2O_5$ glass and the corresponding polycrystalline compound $NaMoO_2PO_4$ (a) and $25Na_2O.50WO_3.25P_2O_5$ glass and the corresponding polycrystalline compound $NaWO_2PO_4$ (b).

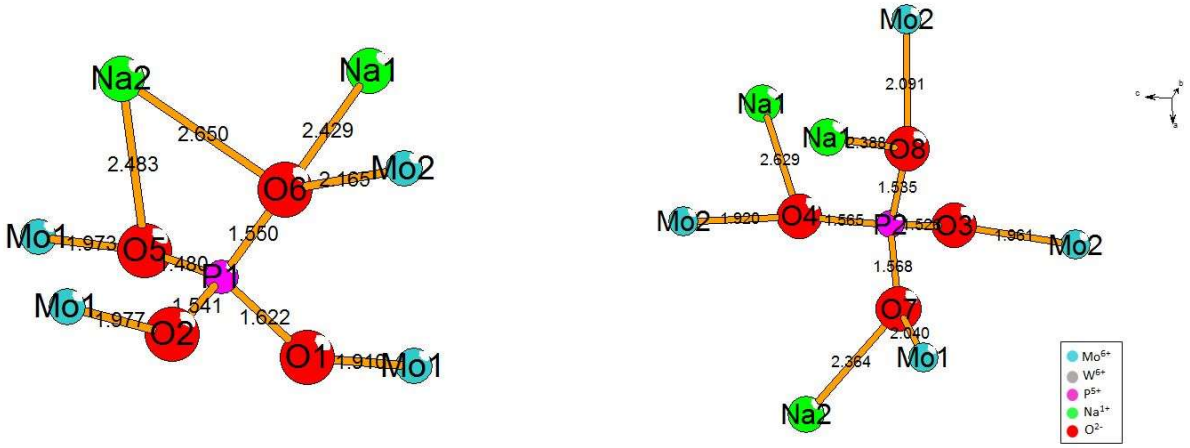

Fig. 9. Short range environment of the P atoms in the $NaMoO_2PO_4$ crystalline compound according to the data of Kierkegaard in Ref. 15.